

Diffusivity and defect reactions of lithium in GaAs

K. Leosson and H. P. Gislason

Science Institute, University of Iceland, Dunhaga 3, IS-107 Reykjavik, Iceland

(Received 13 February 1997; revised manuscript received 6 May 1997)

The diffusion of lithium in GaAs is shown to be trap limited at high doping levels. As in the case of other reactive impurity species in semiconductors, the intrinsic diffusivity of Li in GaAs can only be measured in lightly Li-doped material that has high purity or exhibits weak pairing interactions. From charge-density profiles in Zn-doped GaAs measured by the capacitance-voltage technique we determine the intrinsic diffusivity of Li to be $D_i = D_0 \exp(-E_m/k_B T)$ with $E_m = 0.67 \pm 0.02$ eV and $D_0 = (0.5-2) \times 10^{-2}$ cm²/s. In Li-rich, nominally undoped starting material, however, the diffusion is limited by the formation of complexes involving several Li atoms and native defects. The most weakly bound Li atoms are released from the complexes above 100 °C and a dissociation energy of $E_d = 1.20 \pm 0.03$ eV can be used to characterize the effective diffusion behavior. A previously reported 1.0-eV migration energy for lithium in Li-saturated GaAs at high temperatures is consistent with our observations under the model of trap-limited diffusion. [S0163-1829(97)05839-6]

I. INTRODUCTION

Accurate evaluation of the intrinsic diffusivity of reactive impurity species in semiconductor crystals is a challenging task. Although impurity migration can be studied quite easily, e.g., by means of secondary-ion-mass spectroscopy (SIMS) or charge profiling techniques, some migrating species exhibit a strong tendency to form complexes with other impurities or native defects in the crystal. Elementary analysis of the diffusion kinetics¹ reveals that the diffusion may in some cases be described by the standard diffusion equations, provided that the intrinsic diffusivity is replaced by an effective diffusivity D_{eff} . The modified diffusion coefficient in the presence of trapping centers can then be expressed as

$$D_{\text{eff}} = \frac{D_i}{1 + \frac{4\pi R N D_i}{\nu_d}}, \quad (1)$$

where D_i is the intrinsic diffusivity, R and N denote the capture radius and number of trapping centers, respectively, and ν_d is the complex dissociation frequency. At high temperatures, where $\nu_d \gg R N D_i$, the effective diffusivity equals the intrinsic diffusivity whereas at lower temperatures the defect migration is limited by the complex dissociation frequency.

This simple model was used successfully to account for trap-limited hydrogen diffusion in p -type Si at low temperatures yielding an upper limit of 0.7 eV for the migration energy of H^+ in silicon¹ consistent with a value of around 0.5 eV previously obtained from high-temperature data.² When different charge states of hydrogen, several kinds of trapping centers, and the formation of H_2 molecules are taken into account the analysis becomes more elaborate. Deuterium diffusion profiles in p -type GaAs have been accurately simulated using such a detailed model, suggesting a migration energy around 0.6 eV for H^+ in GaAs.³

Early reports on diffusion of lithium in Si and GaAs indicated similar pairing effects. In the case of silicon, activation energies deduced by Pell⁴ from low-temperature ion-

drift measurements agreed with high-temperature diffusion data only in very pure material where trapping was insignificant, giving values around 0.6 eV (Ref. 4). In contrast to the sensitive ion-drift measurements made on Si samples of very low Li concentrations ($[\text{Li}] \sim 10^{13}$ cm⁻³), diffusion of lithium in GaAs was investigated by Fuller and Wolfstirn⁵ near the solubility limit of Li ($[\text{Li}] \sim 10^{19}$ cm⁻³). In the latter case, the diffusion was described as “dissociative” rather than Fickian. The initial part of the diffusion process was found to be characterized by an activation energy around 1.0 eV. This value has been included in the literature with data on intrinsic diffusion coefficients in GaAs (see, e.g., Refs. 6 and 7). Fuller and Wolfstirn suggested the formation of $\text{Li}_i\text{-Li}_{\text{Ga}}$ and $(\text{Li}_i)_2\text{-Li}_{\text{Ga}}$ complexes but later spectroscopic investigations failed to confirm the existence of such simple configurations, indicating more complicated Li-Li interactions.⁸

This paper presents results of low-temperature annealing experiments yielding activation energies that govern Li migration in p -type GaAs, confirming that lithium diffusion is strongly trap limited in Li-rich material. We derive the intrinsic migration energy of Li in GaAs using similar measurements on material with a low Li concentration and weak pairing interaction. Supporting measurements of localized vibrational modes (LVM's) in Li-diffused material were carried out using Fourier-transform infrared (FTIR) spectroscopy.

II. EXPERIMENT

Samples used in this study were cut from GaAs wafers grown by the horizontal Bridgman method. Two starting materials were used for electrical measurements, nominally undoped GaAs (room-temperature carrier concentration $n = 1 \times 10^{16}$ cm⁻³) and Zn-doped GaAs ($p = 4 \times 10^{16}$ cm⁻³). FTIR measurement were carried out on several different starting materials, ranging from heavily Zn-doped p -type to nominally undoped n -type and semi-insulating starting materials. Samples were diffused with lithium using open-tube diffusion under Ar ambient from arsenic-saturated

gallium melt containing 99.9% Li metal. The doping level was controlled by varying the diffusion temperature, diffusion time, and amount of Li metal in the melt. The diffusion procedure results in a homogeneous Li distribution throughout the bulk of the sample as described elsewhere.⁹

After diffusion, samples were cleaned and etched. For electrical measurements, Schottky diodes with a typical breakdown voltage of 2–3 V were formed on *p*-type material by evaporating 1000 Å of aluminum on the sample surface through a shadow mask of 1 mm diameter. Gold dots of similar dimensions were used on *n*-type material, giving Schottky barriers with a high (>30 V) breakdown voltage. Ohmic contacts were made on the opposite side of the samples by welding Zn or Sn-coated gold wire to the surface of *p*- and *n*-type samples, respectively.

Annealing experiments were carried out under vacuum in a Joule-Thompson refrigeration system. The unit was capable of cooling rates of 0.5 K/s and heating rates exceeding 3 K/s. The stability of the temperature regulator was within 0.1 K in the investigated temperature range. Short annealing times were corrected for the effect of finite cooling and heating rates. Capacitance-voltage [$C(V)$] profiles were measured using a 1-MHz Boonton 72B differential capacitance meter.

FTIR measurements were performed using DA3+ and DA8 Bomem interferometers equipped with a globar light source and mylar beam splitters. The transmitted light was detected with a bolometer. Samples were cooled in CF 204 or CF 1204 Oxford Instruments continuous-flow cryostats to temperatures around 6 K.

III. RESULTS

Previous electrical measurements have shown that Li compensates shallow donors in *n*-type material and passivates the electrical activity of native electron traps.¹⁰ If more lithium is introduced into *n*-type GaAs the material is converted to *p*-type followed by Li self-compensation with the final hole concentration depending on the diffusion conditions. When Li is introduced into *p*-type GaAs it reduces the conductivity and initially increases the hole mobility by forming electrically inactive Li-acceptor pairs.⁹ Heavy Li doping eventually decreases the carrier mobility and renders both *n*-type and *p*-type starting materials semi-insulating.

The interaction of lithium with other impurities and defects in GaAs has been monitored by studying LVM infrared absorption bands that appear when lithium is diffused into the material. Extensive studies of Li-diffused *n*-type material show Li-related LVM's involving native defects⁸ as well as substitutional Si donors.¹¹ Localized modes of lithium paired with most common acceptors in GaAs, such as Mn, Cd, and Zn, have also been investigated.¹²

A. Annealing experiments

Reverse-bias annealing of Schottky diodes was carried out to study the kinetics of defect interactions in our samples. Charge-density profiles were recorded at low temperatures using standard $C(V)$ techniques. The methodology is described in detail by Zundel and Weber.¹³ Samples from nominally undoped starting material that remained *n* type

after Li diffusion exhibited high thermal stability and no change was observed in charge-density profiles after reverse-bias annealing at temperatures up to 200 °C. It may be concluded that the compensating Li resides in relatively stable configurations, presumably bound to native defects as noted in Sec. III B. In *p*-type samples containing Li, however, significant charge transfer is observed after annealing under bias, even below room temperature. Similar behavior was observed previously in Li-passivated Zn-doped and Cu-doped GaAs^{14,15} and attributed to the drift of Li_i^+ ions in the electric field of the reverse-biased junction. When the bias is removed, ions diffuse from the bulk of the material back into the Li-depleted region.

Measurements on acceptor reactivation in Zn-doped starting material have been presented previously.¹⁵ It was shown that Li-passivated Zn acceptors are reactivated upon reverse-bias annealing, even below room temperature. We confirmed that Zn acceptor reactivation in samples used in the present study was governed by the same parameters as previously reported. No transfer of space charge is observed in the *p*-type starting material under similar annealing conditions prior to the introduction of Li. Charge concentration profiles were measured in undoped GaAs starting material, converted to *p* type by Li diffusion at 500 °C for 20 h using the technique described in Ref. 15. The final Hall hole concentration in the sample was around $2 \times 10^{15} \text{ cm}^{-3}$ at room temperature. The total Li content of similarly treated samples has been determined by SIMS measurements⁹ to be of the order of 10^{18} cm^{-3} .

Charge-density profiles were also monitored during zero-bias annealing at different temperatures in order to quantify and compare lithium diffusion parameters. A step in the impurity distribution was created with prolonged reverse-bias annealing and charge-density profiles were recorded periodically during subsequent thermal treatment without bias. The effective diffusivity of Li in GaAs was determined from these measurements as discussed in Sec. IV A.

Space-charge-density profiles in highly Li-diffused GaAs after successive zero-bias annealing treatments are shown in Fig. 1. The initial curve was recorded after annealing with a 2-V bias at 420 K for 3 h. The step in the charge-density profile disappears after annealing without bias for several hours at 420 K as shown in the figure. Similar measurements were carried out in the temperature range 400–490 K.

Zero-bias annealing measurements were also made on Zn-doped starting material passivated with Li. Corresponding space-charge-density profiles are shown in Fig. 2. The sample was diffused with Li at 400 °C for 8 h. Prior to measurement, the sample received a mild heat treatment for a prolonged period of time that removed much of the Li introduced by the diffusion process. Here, the maximum acceptor reactivation in the near-surface region after annealing with a 1.5-V bias for several minutes at 330 K is around $5 \times 10^{15} \text{ cm}^{-3}$, roughly one-fifth of the maximum reactivation observed in heavily Li-diffused undoped starting material, reflecting the different concentrations of mobile Li in the samples. Annealing without bias for several hours at 300 K was sufficient to restore the equilibrium charge distribution. Zero-bias annealing measurements on Zn-doped material were carried out for annealing temperatures between 280 K and 345 K.

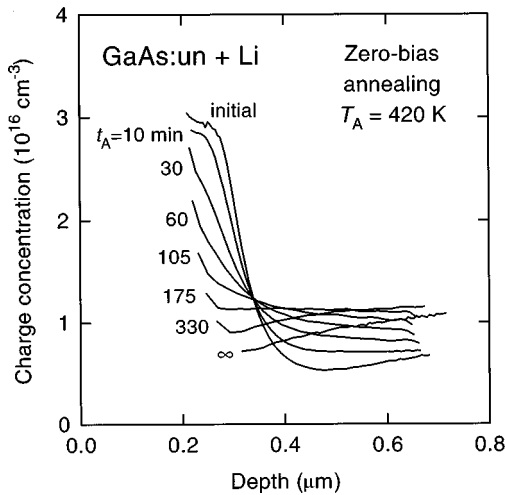


FIG. 1. Charge concentration profiles in Li-rich material during zero-bias annealing. The initial profile was created by annealing with a 2-V reverse bias at 420 K for 3 h. The label “∞” represents a 30-min anneal without bias at 460 K. Profiles were measured at 270 K after rapid cooling of the sample.

B. Li-related localized-vibrational-mode infrared absorption bands

Figure 3 shows absorption spectra of three samples, measured by FTIR spectroscopy. The samples were prepared as follows: highly Zn-doped starting material ($p = 1 \times 10^{19} \text{ cm}^{-3}$) diffused with Li at 800 °C for 9 h (curve A) and at 850 °C for 8 h (curve B) and nominally undoped semi-insulating starting material was Li diffused at 850 °C for 8 h (curve C). In the conducting samples the free-carrier concentration dropped four (curve A) or five (curve B) orders of magnitude after Li diffusion and the carrier mobility increased significantly.

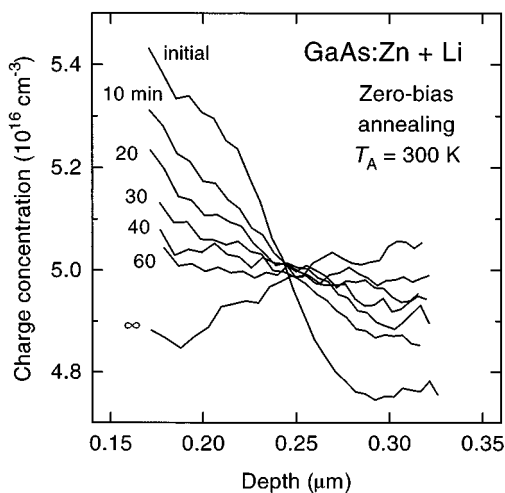


FIG. 2. Space-charge-density profiles measured during zero-bias annealing of lightly Li-passivated Zn-doped starting material. Upon reverse-bias annealing at 330 K for 3 h with a reverse bias of 1.5 V a step is created in the profile (“initial”). During subsequent zero-bias annealing the impurity distribution approaches equilibrium, represented by the “∞” profile, recorded after a 30-min zero-bias anneal at 320 K.

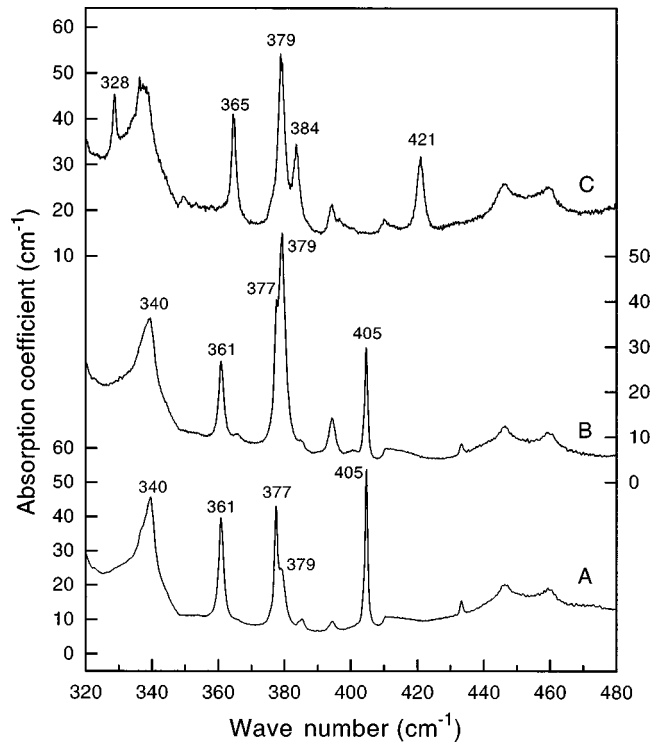


FIG. 3. Absorption spectra in Li-diffused GaAs measured by Fourier-transform infrared spectroscopy. Curves A and B represent Zn-doped starting material with different concentrations of lithium whereas curve C was measured in undoped starting material. The spectral positions of dominating localized vibrational modes are indicated.

Curve A of Fig. 3 is characteristic of GaAs doped with Li and Zn in similar concentrations. Under these circumstances the material is nearly depleted of holes through passivation of the Zn acceptors by Li. Four vibrational modes are consistently observed under such conditions. Their spectral positions are 340, 361, 377, and 405 cm^{-1} (Ref. 12). These modes can be attributed to neutral Zn-Li complexes, since the hole mobility always increases in samples which show this spectrum alone.⁹

Other weak Li-related modes are present in the sample of curve A, the strongest one represented by an absorption peak at 379 cm^{-1} . This mode increases in strength with higher Li concentration, as curve B indicates. Several weaker peaks appear as well but are ignored here. In starting materials with lower Zn concentration, weaker Li doping suffices to produce an LVM spectrum similar to curve B.

If the concentration of Li is increased further the Li-Zn peaks disappear whereas the 379- cm^{-1} peak remains strong and four additional peaks appear, their spectral positions being 328, 365, 384, and 421 cm^{-1} . These five peaks also appear in *n*-type and semi-insulating starting materials containing Li. Curve C is representative of this situation, showing the FTIR spectrum of nominally undoped semi-insulating starting material doped with Li under similar diffusion conditions as the sample of curve B. A decrease in the Hall mobility of free carriers in both *n*- and *p*-type material is observed with the appearance of the five Li-related LVM's. Stronger Li doping always makes these samples semi-insulating, while Li-diffused semi-insulating starting mate-

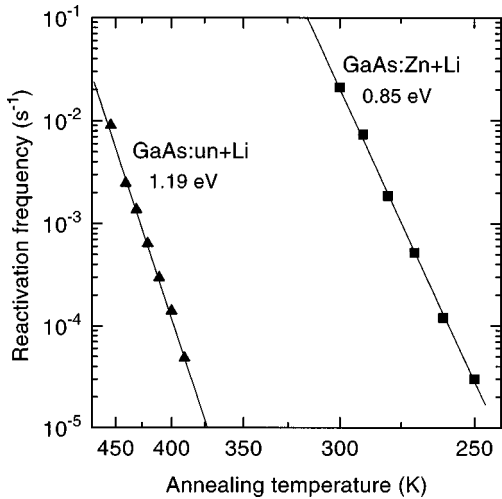


FIG. 4. Arrhenius plot of charge reactivation frequencies in Li-rich GaAs (\blacktriangle). Data from Ref. 15 (\blacksquare) are included for comparison. Activation energies determined by a least-squares linear fit to the data are indicated.

rial remains highly resistive. The LVM spectrum of the different starting materials invariably resembles curve *C* after heavy Li doping.

In early work, the 379-cm^{-1} peak was assigned to a Li-related complex acting as a donor and the peak at 365 cm^{-1} was attributed to a complex acceptor involving Li.⁸ Qualitatively, our observations are in good agreement with these assignments. In particular, the decrease of the Hall mobility agrees with the increased concentration of ionized impurities which act as scattering centers for the charge carriers at high lithium doping levels.⁹ The three remaining peaks were suggested to arise from different neutral defect complexes. Mixed isotope investigation suggests that all of the complexes responsible for the Li-related absorption peaks in curve *C* involve two or more Li atoms in addition to a native defect.⁸

IV. ANALYSIS AND DISCUSSION

A. Complex dissociation and effective diffusivity

Low-temperature impurity migration in compensated semiconductors is commonly governed by defect pairing. Dissociation energies of defect pairs may be derived from reverse-bias annealing data as discussed in Ref. 15. Reactivation frequencies $\nu(T)$ are plotted against reciprocal annealing temperature in Fig. 4. By analogy with previous literature we identify the thermal activation enthalpy with a complex dissociation energy E_d . The preexponential frequency ν_0 depends on the atomic vibrational frequency, number of available adjacent sites, and entropy factors. For hydrogen-related complexes it is generally of the order of 10^{13} s^{-1} (see, e.g., Ref. 16). From our data we deduce $E_d = 1.19 \pm 0.03\text{ eV}$ and a preexponential factor $\nu_0 = (0.5 - 2.5) \times 10^{11}\text{ s}^{-1}$. Figure 4 also includes reactivation frequencies measured in Li-passivated Zn-doped starting material, giving $E_d = 0.85 \pm 0.02\text{ eV}$ and $\nu_0 = (3 - 5) \times 10^{12}\text{ s}^{-1}$, attributed to the dissociation of Li-Zn complexes.¹⁵

Interstitial impurity migration in the absence of an electric field is well represented by the standard diffusion equations,

recognizing the fact that only unpaired atoms diffuse freely through the crystal. Furthermore, the rate of change of the number of complexes must be reflected in the number of free atoms. Therefore,

$$\frac{\partial C_A^f}{\partial t} = D_i \frac{\partial^2 C_A^f}{\partial x^2} - \sigma C_A^f C_B^f + \nu C_{AB}. \quad (2)$$

Here, C_X^f denotes the free concentration of species *X* and C_{AB} is the concentration of complexes. This equation must be solved numerically in order to accurately simulate trap-limited diffusion in the material. Under certain experimental conditions, however, a number of simplifying assumptions can be made and Eq. (2) becomes¹

$$\frac{\partial C_A}{\partial t} = D_{\text{eff}} \frac{\partial^2 C_A}{\partial x^2}, \quad (3)$$

with D_{eff} given by Eq. (1). In this case, the equation has analytical solutions for certain initial conditions. In particular, if the impurity profile can be viewed as a single step function in an infinite medium the solution is given by the complimentary error function, the spatial derivative of which is a Gaussian peak centered at the initial step and decreasing in height as $1/\sqrt{4D_{\text{eff}}t}$. This approach was used in Ref. 1 to extract D_{eff} for hydrogen in Si:B. The spatial restrictions imposed by the low breakdown voltage in our diodes prevent such a simple approximation since the impurity profile can only be recorded in a small region of the sample.

As an alternative approach, the initial impurity profile was approximated with a series of step functions and symmetrized around the edge of the zero-bias depletion region in order to prohibit diffusion against the built-in electric field. The resulting solution to Eq. (3) can be written as $C_A(x, \lambda)$ where λ is the diffusion length $\sqrt{4D_{\text{eff}}t}$. Analogous to Ref. 1 we introduce the parameter $s(x, \lambda) = -\partial C_A / \partial x$. In our case, the reciprocal peak height $1/s_p$ is not a linear function of λ .

The derivative $s(x, t)$ was determined from the experimental data by subtracting the final charge-density profile ($t \rightarrow \infty$) from the profile measured at a given time *t* and differentiating the result with respect to *x*. The effective diffusivity at each annealing temperature was deduced from $s_p(t)$ by scaling the time variable of the $1/s_p(t)$ data to fit the calculated $1/s_p(\lambda)$ curve. Results are shown in Fig. 5 for the Li-rich material. The scaling factors $D_{\text{eff}}(T)$ used to match calculated and measured values at each temperature are indicated in the figure. Analogous calculations were performed for the lightly Li-diffused, Zn-doped starting material.

B. Determination of the intrinsic diffusion coefficient

Effective diffusivities determined from the zero-bias annealing data presented above are plotted as a function of reciprocal temperature in Fig. 6. Also included in the figure are results of the high-temperature diffusion experiments of Fuller and Wolfstirn.⁵ Activation energies determined from the present data are $1.20 \pm 0.03\text{ eV}$ for Li-rich material and $0.75 \pm 0.02\text{ eV}$ for Zn-doped starting material. The former agrees, within experimental uncertainty, with the complex dissociation energy measured by reverse-bias annealing. In

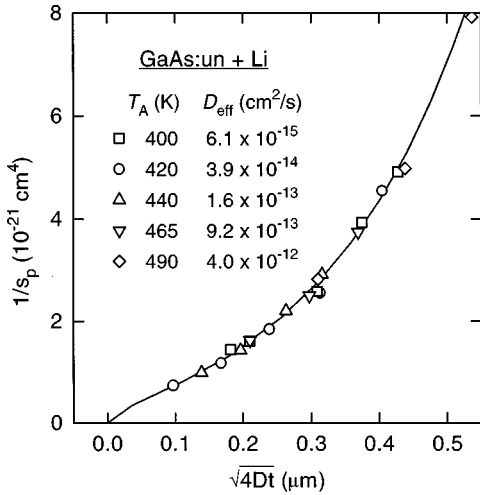


FIG. 5. Annealing parameter $1/s_p$ determined from charge-density profiles during zero-bias annealing at different temperatures. The annealing times are scaled to match the theoretical curve (solid line). The scaling parameters D_{eff} for each temperature are indicated.

the latter case, however, the activation energy deviates from the 0.85-eV dissociation energy measured in Li-passivated Zn-doped starting material.

Using dissociation frequencies of Li-Zn complexes from Ref. 15 and assuming that the total number of trapping centers in the Zn-doped material equals the shallow acceptor concentration, $N = 4 \times 10^{16} \text{ cm}^{-3}$, we can determine the intrinsic diffusivity D_i from Eq. (1). The capture radius of shallow (hydrogenlike) centers equals 3–5 nm in GaAs at temperatures used in the present work.³ The derived values of D_i are included in Fig. 6. In Li-rich material the impurity migration is controlled by the 1.20-eV complex dissociation

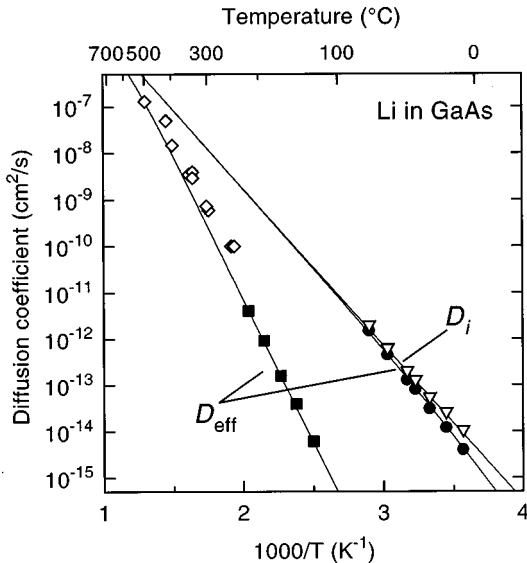


FIG. 6. Arrhenius plot showing effective diffusion coefficients determined in Li-rich GaAs (■) and weakly Li-doped GaAs:Zn (●). High-temperature diffusion data from Ref. 5 are included (◇). Calculated values of D_i (▽) were determined from the effective diffusivity measured in Zn-doped starting material. Solid lines represent theoretical curves for intrinsic and effective diffusivities in the two materials.

energy, in accordance with these results and Eq. (1). A least-squares fit through the calculated values of D_i gives

$$(D_i)_{\text{Li}} = (1_{-0.5}^{+1.0} \times 10^{-2}) \exp\left(\frac{-0.67 \pm 0.02 \text{ eV}}{k_B T}\right) \text{ cm}^2/\text{s}. \quad (4)$$

In the above analysis, D_i is determined from D_{eff} by assuming (a) that the diffusion follows Eq. (3) and (b) that D_{eff} is given by Eq. (1). The validity of these assumptions was verified by numerically solving Eq. (2) with an additional self-consistent electric-field term allowing for the drift of charged Li. Initial conditions were calculated for the given bias conditions and concentration profiles determined for several annealing times after external bias was lifted. Calculations were carried out for the Li-Zn system at two temperatures, representing the boundaries of the experimental annealing range, using values of D_i given by Eq. (4). Numerically simulated concentration profiles agreed well with the analytical solutions and the discrepancy between the effective diffusivities was less than 5% at 330 K and less than 20% at 280 K. The possible error in the calculated intrinsic diffusivity due to assumptions (a) and (b) is within the quoted uncertainty limits of D_i . In the Li-rich material Eq. (1) with $N \approx 4 \times 10^{15} \text{ cm}^{-3}$ provides a good fit to the experimental data.

C. Comparison with previous literature

The 0.67-eV migration energy determined from our data agrees with commonly observed values (0.5–0.7 eV) for interstitial diffusion.¹⁷ The prefactor D_0 is close to measured values for hydrogen² and lithium⁴ in silicon. The diffusion data of Fuller and Wolfstirn⁵ agree fairly well with our measurements on heavily Li-doped material despite the difference in starting materials, diffusion temperature, and method of extracting D_{eff} . Exact agreement is not expected since the assumption is that the trapping process depends on the total Li concentration as well as the concentration and nature of native defects in the material. However, based on the present results and the model of trap-limited diffusion, we expect diffusivity measurements above 300 °C to yield intermediate activation energies between E_m and E_d . The previously reported 1.0-eV activation energy⁵ is consistent with our value of E_m and defines a lower limit for the dissociation energy of Li-related complexes in samples used in that study.

The value of E_m deduced from our data also correlates well with a model put forward in a recent review on emission channeling studies of Li in semiconductors,¹⁸ stating that the migration energy can be expressed in terms of the time needed for implanted ⁸Li to combine with Ga vacancies created during the implantation process. A detailed analysis of the recombination kinetics yields a migration energy around 0.6 eV (Ref. 18).

V. CONCLUSIONS

As in the case of atomic hydrogen, the intrinsic diffusion coefficient rarely characterizes the migration of Li in GaAs due to its strong tendency to react with other defects. We have demonstrated that in highly Li-doped material, complexes containing native defects and several Li atoms are

formed, heavily retarding the migration of Li through the crystal. In our samples, a limited amount of lithium can be released from such complexes provided that a dissociation energy barrier of 1.20 eV is surmounted. This value is assumed to represent the weakest Li-complex bond in the material and is likely to depend on the total amount of Li in the sample as well as the nature of the starting material. This issue was not pursued further in the present work since the main focus was on determining the intrinsic diffusivity of Li.

In Li-passivated Zn-doped material the lithium is mainly paired with Zn acceptors, even to moderately high Li-doping levels, as demonstrated by FTIR measurements. At low doping levels there is only minimal indication of the association of Li and native defects. Ion-drift measurements on such samples reveal a much weaker pairing interaction than observed in Li-rich material and the original acceptor concentration is easily recovered in the near-surface region by driving Li toward the bulk of the samples with the application of an electric field. The activation energy for the effective diffusion coefficient in this case is lower than the measured dissociation energy, indicating that the pairing interaction is not a limiting factor in the diffusion kinetics. Values of D_i

were determined from the effective diffusivity using the model of trap-limited diffusion, and the self-consistency of this approach was verified by numerical calculations.

We conclude that Eq. (4) is the most accurate expression available for the diffusion coefficient of interstitial lithium in GaAs. In order to obtain more complete data, the effective diffusion coefficient must be measured above 100 °C in a weakly interacting system. In this case, the field drift of Li ions is too fast to be followed by the sequential bias annealing and space-charge profiling technique employed here and other methods of extracting D_{eff} are called for.

ACKNOWLEDGMENTS

The authors wish to thank B. H. Yang for sample preparation and L. Zunkowski for assisting with the electrical measurements. We are grateful to B. Clerjaud, A. Lebkiri, A. Mari, and C. Naud for assistance in the optical-absorption measurements. This research was partially supported by the Icelandic Council of Science and the University Research Fund.

¹T. Zundel and J. Weber Phys. Rev. B **46**, 2071 (1992).

²A. Van Wieringen and N. Warmholtz, Physica (Utrecht) **22**, 849 (1956).

³R. Rahbi *et al.*, Physica B **170**, 135 (1991).

⁴E. M. Pell, J. Appl. Phys. **31**, 291 (1960).

⁵C. S. Fuller and K. B. Wolfstirn, J. Appl. Phys. **33**, 2507 (1962).

⁶S. M. Sze, *Physics of Semiconductor Devices* (Wiley, New York, 1981), p. 68.

⁷A. G. Milnes, Adv. Electron. Electron Phys. **61**, 63 (1983).

⁸M. E. Levy and W. G. Spitzer, J. Phys. C **6**, 3223 (1973).

⁹B. H. Yang, H. P. Gislason, and M. Linnarsson, Phys. Rev. B **48**, 12 345 (1993).

¹⁰T. Egilsson, B. H. Yang, and H. P. Gislason, Phys. Scr. **T54**,

28 (1994).

¹¹W. M. Theis and W. G. Spitzer, J. Appl. Phys. **56**, 890 (1984).

¹²O. G. Lorimor and W. G. Spitzer, J. Appl. Phys. **38**, 3008 (1967).

¹³T. Zundel and J. Weber, Phys. Rev. B **39**, 13 549 (1989).

¹⁴H. P. Gislason, T. Egilsson, K. Leosson, and B. H. Yang, Phys. Rev. B **51**, 9677 (1995).

¹⁵K. Leosson, B. H. Yang, and H. P. Gislason, Mater. Sci. Forum **196-201**, 1395 (1995).

¹⁶S. J. Pearton, C. R. Abernathy, and J. Lopata, Appl. Phys. Lett. **59**, 3571 (1991).

¹⁷B. Tuck, *Atomic Diffusion in III-V Semiconductors* (Hilger, Bristol, 1988).

¹⁸U. Wahl, Phys. Rep. **280**, 145 (1997).